Gene Expression Profiling in Rat Liver After VMH Lesioning

TAKAYOSHI KIBA,* YURI KINTAKA,* YOKO SUZUKI,* EIKO NAKATA,* YASUHITO ISHIGAKI,† AND SHUJI INOUE*,[1]

*Laboratory of Clinical Nutrition & Physiology, Kyoritsu Women's University, Tokyo 101-8433, Japan; and †RI Center, Kanazawa Medical University, Ishikawa 920-0293, Japan

It has been reported that ventromedial hypothalamic (VMH) lesions induce hepatic cell proliferation and apoptosis and metabolic changes in the body. In the present study, we identified genes of which expression profiles showed significant modulation in rat liver after VMH lesions. Total RNA was extracted, and differences in the gene expression profiles between rats at day 3 after VMH lesioning and sham-VMH lesioned rats were investigated using DNA microarray analysis. The results revealed that VMH lesions regulated the genes that were involved in various types of metabolisms and cell proliferations in the liver. Real-time PCR also confirmed that gene expressions of ELOVL6 and SPC24 were upregulated, and that of SERPINA7 was downregulated. VMH lesions may change the expressions of multiple metabolism genes and cell proliferation–related genes in rat liver. Exp Biol Med 234:758–763, 2009

Key words: VMH; gene expression; cell proliferation and apoptosis; metabolism; liver; rat

Introduction

A focus of attention among researchers has been the pathways that connect the nervous system and the gastrointestinal organs (1, 2). The liver is one of the autonomic nerve–enriched organs (1, 2). The hypothalamus plays a vital role in the integration of neurohumoral information and possesses autonomic centers that are connected to the viscera via the autonomic nervous system (1, 2). It is well known that VMH lesions change various types of metabolisms in the body (3). We previously reported that VMH lesions induce hepatic cell proliferation and apoptosis (4, 5).

DNA microarray analysis is a powerful tool for detecting the characterization of mRNA expression pattern of a large number of genes. In the present study, we used DNA microarray analysis to identify genes for which expression profiles showed significant modulation and to investigate the cellular mechanisms of gene regulation in the rat liver at day 3 after VMH lesions, because it has been reported that cell proliferation in the liver increases and reaches a maximum at day 3 (4), and real-time polymerase chain reaction (PCR) also confirmed a part of the results obtained by DNA microarray analysis.

Materials and Methods

Female Sprague-Dawley rats weighing 230–250 g were used in this study. They were maintained in a constant-temperature environment (23 ± 2°C) in light-controlled cages with a 12-h light-dark cycle (lights on 7:00 AM) and were given free access to food and water. Tissue samples were taken from the liver of VMH-lesioned rats and sham VMH-lesioned rats at day 3 after the operation ($n = 2$ in each group for DNA chips and $n = 3$ in each group for real-time polymerase chain reaction).

VMH lesions or simulated operations were performed as previously described (4–6). The stereotaxic coordinates were at bregma anteriorly, 0.75 mm lateral to the midsagittal line, and 1.0 mm upward from the base of the skull, according to the atlas of De Groot (7). Sham operations were performed in an identical manner, except that no current was applied. After the operations, the rats were returned to their cages and given free access to food and water. Localization of the VMH lesions was verified by

All authors have stated that there is no conflict of interest to disclose regarding the information in this manuscript.

The accession numbers for information regarding the microarray are: 1367707_at; 1367856_at; 1367904_at; 1368160_at; 1368883_at; 1369455_at; 1369531_at; 1370067_a; 1370269_at; 1370334_at; 1371143_at; 1371237_a_at; 1373026_at; 1386637_at; 1387123_at; 1387391_at; 1387967_at; 1388108_at; 1388194_at.

[1] To whom correspondence should be addressed at Laboratory of Clinical Nutrition & Physiology, Kyoritsu Women's University, 2-2-1 Hitotsubashi Chiyoda-ku, Tokyo, 101-8433, Japan. E-mail: takkiba@hotmail.com

Received January 22, 2009.
Accepted April 7, 2009.

DOI: 10.3181/0901-RM-30
1535-3702/09/2347-0758$15.00

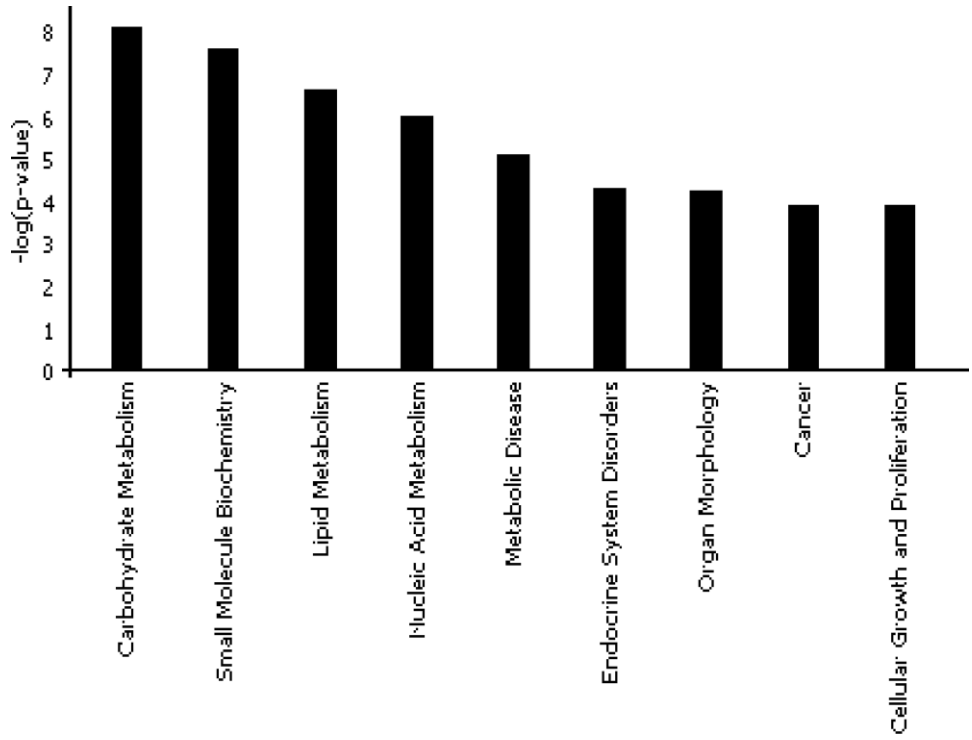

Figure 1. Changed biofunction after VMH lesioning identified in Ingenuity Pathways Analysis.

microscopic examination of the brain at the end of the experiment.

In 2 individual rats at day 3 after VMH lesioning and 2 sham-VMH lesioned rats, in order to circumvent RNA lysis by RNases that may be released in the rat liver when the animal is stressed, all procedures were conducted as swiftly as possible after each rat was sacrificed. The abdominal and chest cavities were opened. The samples of liver were quickly placed in 10 volumes of RNAlater® (Ambion, Inc., Austin, TX) at room temperature. The distance between the tissue surface, which is exposed to preservative, and the innermost regions of the fragment was minimized. We did this by cutting the tissues into 2-mm thick slices, thereby reducing the diffusion distance to 1 mm or less. RNA was isolated from the rat liver, using a commercially available kit (RNA easy Mini Kit, QIAGEN GmbH, Hilden, Germany). The RNA was quantified spectrophotometrically at 260/280 nm, and the quality of the isolated total RNA was determined by electrophoretic separation on anthodium bromide–containing 1% agarose gel. The preparation of cRNA was carried out by Ambion's MessageAmp® II-Biotin Enhanced and the target hybridization was performed according to the instructions provided in the Affymetrix GeneChip® technical manual. The double-stranded cDNA was synthesized from 5 μg of total RNA and hybridized Affymetrix GeneChip® arrays (Rat Genome 230 2.0, Affymetrix Japan Co., Tokyo, Japan) for 16 h at 45°C in a GeneChip® Hybridization Oven 640. After washing and staining in a GeneChip® Fluidics Station 450, hybridized cRNA was detected by a GeneChip® scanner 3000. The digitized image data were processed using the GeneChip® Operating Software 1.4. The amount of probe-specific transcripts was determined based on the average of the differences between the perfectmatch and mismatch intensities. As replicate assays were not performed, a very stringent cutoff point was selected for the detection of significant upregulation or downregulation of the genes in the mRNA amount between the arrays. Using the signal intensity of selected genes that were up- or downregulated compared to the sham-VMH lesioned control group, the analysis was performed using GeneSpring GX 7.3.1 (Agilent Technologies, Santa Clara, CA) and Ingenuity Pathway Analysis (http://www.ingenucity.com/) (Redwood City, CA). Using a computational tool, Ingenuity Pathway Analysis, we were able to build networks of interacting genes from protein-related genes lists.

Regarding the real-time PCR analysis, RNA was stored at –70°C until this analysis was performed. An aliquot (1 μg) of extracted RNA was reverse-transcribed into first-strand complementary DNA (cDNA) at 42°C for 15 min, using 200 U/μl reverse-transcriptase (Takara Biochemicals, Shiga, Japan) and 10 mM of oligo (dT)-adapter primer (Takara Biochemicals) in a 2.0-μl reaction mixture.

Real-time PCR was carried out with a Terminal Cycle Dice TP800 (Takara Biochemicals) using the DNA-binding dye SYBR Green I for the detection of PCR products. The reaction mixture (RT-PCR kit, Code RRO43A, Takara Biochemicals) contained 12.5 μl SYBR Premix Ex Taq (2x) (Code RRO41A, Takara Biochemicals), 10 μM PCR Forward Primer (0.5 μl), 10 μM PCR Reverse Primer (0.5

Table 1. Main Changed Gene Networks at 3 Days After VMH Lesioning Identified in Ingenuity Pathways Analysis[a]

Genes	Score	Focus genes	Top functions
AACS, ABCG5, ACACA, ACLY, AKR1C3, CSAD, ELOVL6, FABP5, FADS2, FASN, G6PD, GPAM, HMGCR, Insulin, IRS3, LSS, ME1, MVD, MYBL1, N-cor, NCOR-LXR-Oxysterol-RXR-9 cis RA, NFkB, ONECUT1, PFKFB1, Pka, PKLR, PP2A, SCD2, SLC2A5, SREBF1, T3-TR-RXR, TMEM97, TNFRSF9, TNFRSF13C, ZMYND1	56	28	Lipid Metabolism, Nucleic Acid Metabolism
ACAT2, Akt, AMPK, Ap1, ASCL1, BHLHB2, CAST, Creb, EFNA1, FGFR1, GPI, Gsk3, HSPB1, Igfbp, IGFBP1, IGFBP2, IL1, IRS2, Jnk, LDL, MEOX2, MT1E, NOV, Pdgf, PDGF BB, PER2, PI3K, Pkc(s), PPAP2B, PVR, S100G, Tgf beta, TGFBR1, VitaminD3-VDR-RXR, ZNF14	35	20	Endocrine System, Metabolism, Reproductive System
Ahr-aryl hydrocarbon-Arnt, AKT1, ASNS, Calmodulin, Caspase, CDKN1A, CISH, CYP1A1, DLAT, E2f, FAM33A, GADD45G, GPX2, Histone h3, HNF4A, ING5, JMJD2C, LDB3, Mapk, NFE2, NOC2L, NUSAP1, P38 MAPK, PFTK1, PTP4A3, RACGAP1, Rb, RNA polymerase II, SUPT16H, TESK1, TPX2, TRIP11, VAMP8, WNT3,WNT4	24	15	Cell Cycle, DNA Replication, Recombination, and Repair, Apoptosis
ALDH1A1, ANKRD25, ATAD2, C12ORF5, Ca2+, CASP3, CCNG1, CDH13, CDKN2A, CDKN2D, CHMP4C, CLCA1 (includes EG:1179), CTCF, CTNNB1, DDR1, dihydrotestosterone, ELL, EMILIN2, FZD7, GSTA3, HEMGN, HNRNPA2B1, IL10, ME1, PDCD6IP, PLA2G12A, progesterone, S100A11 (includes EG:6282), SPTBN1, STK11, TKT, TMEM97, TP53, TP53INP1, ursodeoxycholic acid	24	15	Apoptosis, Cell Growth and Proliferation
ALPL, ARF1, ATF4, BMF, CALR, CREB1, FGL2, GBP4 (includes EG:115361), GJA5,GTP, HACL1, HNF1A, IFNG, KRT19, LGALS8, MAPK8, MAPT, melatonin, MMP11, ODC1, PGD, PLEKHB1, PSPH, retinoic acid, RPL11, SCUBE1, SCYE1, SEC63, SERPINA7, SRP54, SYT9, TCF7L2, TGM1, thyroxine, TNFAIP6	22	14	Cell Growth and Proliferation, Apoptosis
ATAD2, ATP, ATPIF1, beta-estradiol, CCNE2 (includes EG:9134), CDC6, COMMD6, CTSD, ELN, estrone, IFI30, INHBE, KLF4, KLF10, KRT19, ORC1L, PKIB, PPCS, PRKCH, PTP4A1, RELA, RESP18, SKIP, SLC39A4 (includes EG:55630), SMARCA4, SOD2, sulfotransferase, SULT1A3, SULT1C2, SULT4A1, TERT, TMEM164, Ubiquitin, ZRANB1	20	13	Cell Growth and Proliferation, DNA Replication, Recombination, and Repair
BCL3, CAPRIN1, CDC42SE1, CTSC, DUSP22, E2F4, EVL, FGF2, GUSB, HRAS, HSD11B1, IL13, MAPK1, MKI67, NDC80, NUF2, ODC1, OPN3, PIR, POLA2, PRC1, RPL39, RSU1, SMC2, SMC4, SPC24, SPC25, SPINK1 (includes EG:6690), SRF, TGFB1, TNF, TNNT2, TPST1,TTK, ZWINT (includes EG:11130)	20	13	Cell Cycle, Cellular Development
2-methoxyestradiol, AGER, AP3D1, BUB1 (includes EG:699), CDC6, CDC25C, COPZ1, CTTN, CYP1A1, EDG7, EGFR, EZH1, FOXM1, GADD45B, GALE, GARNL1, hydrogen peroxide, ID3, IL6, IL1R1, INSR, LGALS1, MAD2L1, MCM2, MMP8, NLK, OSGIN1, POU2AF1, RUFY1, SDS, SNX4, TCF3, TMEM55A, TXN, XBP1	16	11	Cell Cycle, Cell Growth and Proliferation, Apoptosis
AGRN, ANGPT1, BZW2, CASP10, CCL2, CCND3, CHD2, Cyclin A, CYP17A1, DIXDC1, DUSP1, DVL2, FGF7, FOXO1, HGF, HMGA1, ID1, IL9, KITLG (includes EG:4254), MAP2K1, Mek, MUSK, NR4A1, NR5A1, NRG1, PDGF-AA, PIM1, PPP2R2A, PTTG1, RAF1, RB1, SPRY2, TSC22D3, USF2, VEGFC	6	5	Cell Growth and Proliferation, Cell Cycle

[a] Note: Ingenuity Pathways Analysis calculates a significance score for each network. (http://www.ingenuity.com/products/Monarch.NovelMolecularMechanisms_high.pdf). The score is generated using a *P* value calculation and is displayed as the negative log of that *P* value. This score indicates the likelihood that the assembly of a set of focus genes in a network could be random chance alone.

Table 2. Upregulated (>5.0 folds) and Downregulated (>4.5 folds) Genes Identified by DNA Microarray Analysis at 3 Days After VMH Lesioning

Accession No.	Gene name	Fold change[a]	Categories	Functions
1) Upregulated genes				
1370269_at	CYP1A1	25.31	Metabolism	Cytochrome P450 enzyme
1388108_at	ELOVL6	17.76	Metabolism	Elongase of long chain fatty acids
1373026_at	SPC24	14.93	Migration	NDC80 kinetochore complex component
1387123_at	CYP17A1	10.41	Metabolism	Cytochrome P450 enzyme
1388194_at	DLAT	6.48	Enzyme	Putative dihydrolipoamide acetyltransferase
1370067_at	ME1	6.33	Metabolism	Cytosolic, NADP-dependent enzyme that generates NADPH for fatty acid biosynthesis
1387967_at	SPINK1	6.10	Metabolism	Trypsin inhibitor to protect the pancreas from premature activation of pancreatic juice; monitor peptide activity to induce cholecystokinin release in the intestine
1367707_at	FASN	6.05	Metabolism	Fatty acid synthase
1367856_at	G6PD	5.23	Metabolism	Glucose-6-phosphate dehydrogenase
2) Downregulated genes				
1371143_at	SERPINA7	–58.08	Enzyme	Serpin peptidase inhibitor
1368160_at	IGFBP1	–12.51	Growth	Insulin-like growth factor binding
1387391_at	CDKN1A	–10.62	Differentiation	Potent cyclin-dependent kinase inhibitor
1371237_a_at	MT1E	–7.10	Binding	Capacity to bind both physiological and xenobiotic heavy metals through the thiol group of its cysteine residues
1369531_at	SULT1C2	–6.68	Enzyme	Sulfotransferase for categorizing sulfate conjugation of many hormones, neurotransmitters, drugs, and xenobiotic compounds
1370334_at	PLEKHB1	–5.80	Morphology	Pleckstrin (a protein found in platelets) homology domain containing
1368883_at	NOV	–5.00	Differentiation	Regulating the proliferation, differentiation, and adhesion
1367904_at	RESP18	–4.95	Signaling	Regulated endocrine-specific protein 18 (a role as an intracellular signaling molecule expressed exclusively in peptidergic neurons and endocrine cells)
1386637_at	FGL2	–4.89	Secretion	Secreted protein that is similar to the beta- and gamma-chains of fibrinogen
1369455_at	ABCG5	–4.70	Transporter	ATP-transporter family member that regulates absorption of dietary cholesterol

[a] Note: Fold changes in average difference values were calculated using Ingenuity Pathway Analysis.

μl), and cDNA (2.0 μl) to give a final reaction volume of 25 μl. The sequences were obtained using Perfect Real Time support system (http://www.takara-bio.co.jp/prt/imtro.htm). The PCR settings were as follows: the initial denaturation for 10 s at 95°C was followed by 40 cycles of amplification for 5 s at 95°C and 30 s at 60°C, with the subsequent melting curve analysis increasing the temperature from 60°C to 95°C. Relative quantification of gene expression with real-time PCR data was calculated relative to GAPDH.

In the present study, 3 representative genes related to metabolism and cell proliferation were investigated by real-time PCR: 1) ELOVL6 (elongation of very long chain fatty acids–like 6); 2) SPC24 (spindle pole body component 24); and 3) SERPINA7 (serpin peptidase inhibitor, clade A, member 7).

Results are expressed as the mean ± SEM. The mRNA levels were analyzed by the Mann-Whitney *U* test. Statistical analysis was conducted with SPSS version 11.0 statistical software. The differences between the groups were considered significant if the *P* value was <0.05 (2-tailed).

Results

Among 31,099 probes, the expression of 203 probes (0.7%) showed at least a 2-fold upregulation (127 probes) or downregulation (76 probes) at day 3 after VMH lesioning as compared with sham-VMH lesioning. Figure 1 shows the changed biofunction after VMH lesioning identified in Ingenuity Pathways Analysis. The result revealed that VMH lesions regulated some genes that are involved in carbohydrate metabolisms, lipid metabolisms, nuclear acid metabolisms, organ morphology, cell growth and proliferation, and so on. Table 1 shows the main changed gene networks at 3 days after VMH lesioning identified in Ingenuity Pathways Analysis. Moreover, Table 2 shows the upregulated and downregulated genes identified by DNA microarray analysis. As to the gene expressions regarding metabolism, VMH lesions upregulated Cytochrome P450, family 1, subfamily A, polypeptide 1 (CYP1A1), elongation

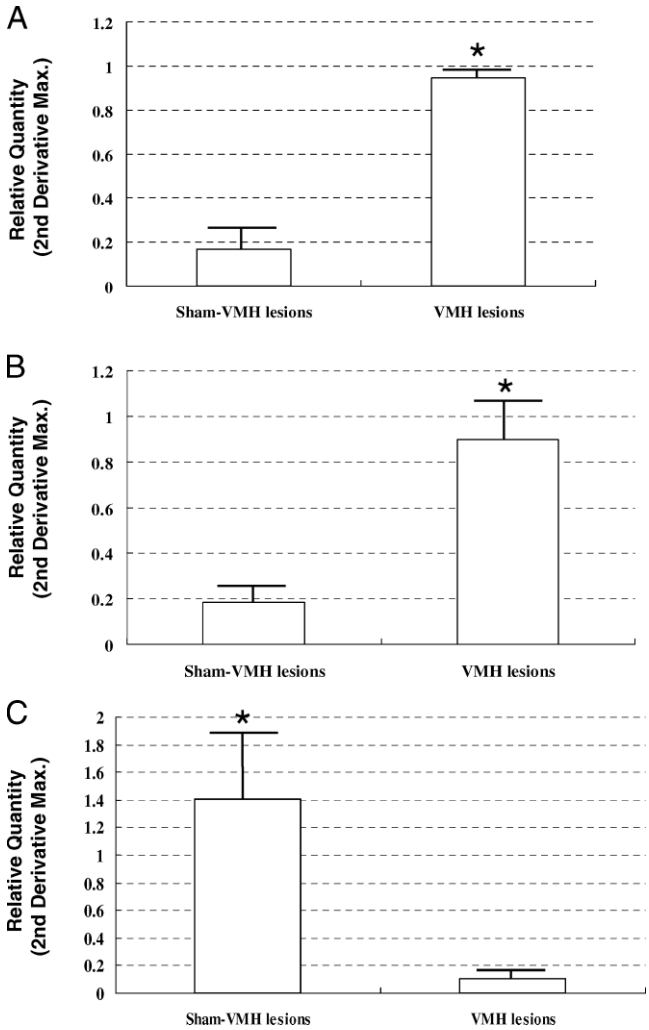

Figure 2. VMH lesion-induced gene expression in real-time PCR analysis. Real-time PCR analysis of total RNA extracts was described in Materials and Methods. A. ELOVL6, elongation of very long chain fatty acids–like 6; B. SPC24, spindle pole body component 24; C. SERPINA7: serpin peptidase inhibitor, clade A, member 7. Values are the means ± SEM of 3 different experiments. * < 0.05 compared with sham-VMH lesioned rats.

of very long chain fatty acids–like 6 (ELOVL6), Cytochrome P450, family 17, subfamily A, polypeptide 1 (CYP17A1), Dihydrolipoamide S-acetyltransferase component of pyruvate (DLAT), Malic enzyme 1, NADP(+)-dependent, cytosolic (ME1), serine peptidase inhibitor, Kazal type 1 (SPINK1), fatty acid synthase (FASN), and glucose-6-phosphate dehydrogenase (G6PD), and downregulated serpin peptidase inhibitor, clade A, member 7 (SERPINA7), sulfotransferase family, cytosolic, 1C, member 2 (SULT1C2), fibrinogen-like protein 2 (FGL2), and ATP-binding cassette, subfamily G, member 5 (ABCG5). Meanwhile, as to gene expressions regarding cell proliferation, VMH lesions upregulated spindle pole body component 24 (SPC24), and downregulated insulin-like growth factor binding protein 1 (IGFBP1), cyclin-dependent kinase inhibitor 1A (CDKN1A), nephroblastoma overexpressed gene (NOV), and regulated endocrine-specific protein 18 (RESP18). The expressions of EVOVL6, SPC24, and SERPINA7 were also examined by the real-time quantitative analysis (Fig. 2). The gene expressions of EVOVL6 and SPC24 were upregulated ($P < 0.05$ and $P < 0.05$, respectively), and that of SERPINA7 was downregulated ($P < 0.05$).

Discussion

In the present study, we used the DNA microarray technique for mRNA expression profiling of rat liver mixtures to investigate cellular responses in response to VMH lesions. The DNA microarray analysis revealed that VMH lesions regulated some genes that are involved in the functions, such as carbohydrate metabolisms, lipid metabolisms, nuclear acid metabolisms, organ morphology, cell growth and proliferation, and apoptosis (Figs. 1 and 2). This result by DNA microarray technique confirmed the previous results that VMH lesions change various types of metabolisms, and that they also induce cell proliferation and apoptosis (4, 6).

As to the genes' expressions regarding metabolism, Table 2 shows the dynamic biofunctional changes of gene expressions. Especially, cytochrome P450 is noted to be changed massively after VMH lesioning. Cytochrome P450 is primarily membrane-associated proteins, located either in the inner membrane of mitochondria or in the endoplasmic reticulum of cells (8). Most cytochrome P450 can metabolize multiple substrates, and many can catalyze multiple reactions, which accounts for their central importance in metabolizing the extremely large number of endogenous and exogenous molecules (8). Consistent with this, Inui et al. (9) previously reported that the content of cytochrome P450 per mg microsomal protein in VMH lesioned rats was significantly higher than that in sham-lesioned rats. Moreover, in the present study, the gene expressions of ELOVL6 and SPC24 were upregulated after VMH lesioning. The upregulation of ELOVL6 gene expression may be involved in developing hepatosteatosis by VMH lesioning (10), because ELOVL6 gene protein is long-chain fatty-acyl elongase and is involved in fatty acid biosynthesis (11). Meanwhile, because the 4-subunit NDC80 complex, which is included in SPC24 protein, directly connects kinetochores to spindle microtubules, SPC24 plays a major role in regulating cell division (12, 13). We previously reported that VMH lesions induce hepatic cell proliferation (4, 5). The changes of SPC24 expression after VMH lesioning confirmed this fact.

We previously reported that VMH lesions induce cell proliferation, but also stimulate Fas/Fas ligand system–mediated apoptosis through the activation of caspase 3 in the rat liver (6). Therefore, VMH lesions may suppress mainly the caspase-dependent type I pathway for apoptosis in the liver. Consistent with this, in the present study, DNA microarray analysis indicated VMH lesions induced the

increased Fas, caspase 3, glutamic-oxaloacetic transaminase (GOT) and glutamic-pyruvic transaminase (GPT) gene expression in liver tissue mixture, but the expression of these probes showed <2-fold upregulation. However, in the present study, the gene expression of SERPINA7, a serpin peptidase inhibitor, was downregulated after VMH lesioning. Because serpins protect hepatocytes from apoptosis mediated by the granzyme-perforin mechanisms present in the abundant natural killer cell found in normal liver (14), and serpins also inhibit metacaspase-like proteases *in vivo* and control cell death pathways (15), the downregulation of SERPINA7 gene expression may protect hepatocytes from apoptosis, and therefore induce cell proliferation in the liver.

In conclusion, many genes related to the changed metabolism and cell proliferation and apoptosis based on VMH lesions were detected by the DNA microarray analysis. Although the networks of these genes involved in this process have not yet been elucidated sufficiently, this study is the first report to demonstrate that VMH lesions may cause changes of various gene expressions regarding metabolism and cell proliferation and apoptosis in the liver.

1. Kiba T, Tanaka K, Inoue S, Endo O, Takamura Y. Comparison of DNA contents of visceral organs in rats with ventromedial hypothalamic lesions and fed a high fat diet. Neurosci Lett 126:127–130, 1991.
2. Kiba T. The role of the autonomic nervous system in liver regeneration and apoptosis—recent developments. Digestion 66:79–88, 2002.
3. Bray GA, York DA. Hypothalamic and genetic obesity in experimental animals: an autonomic and endocrine hypothesis. Physiol Rev 59:719–809, 1979.
4. Kiba T, Tanaka K, Endo O, Inoue S. Role of vagus nerve in increased DNA synthesis after hypothalamic ventromedial lesions in rat liver. Am J Physiol 262:G483–G487, 1992.
5. Kiba T, Tanaka K, Numata K, Saito S, Sekihara H. Hepatocyte proliferation in rats after ventromedial hypothalamic lesions: immunoreactivity patterns of proliferating cell nuclear antigen (PCNA). J Gastroenterol 33:523–528, 1998.
6. Kiba T, Saito S, Numata K, Kon Y, Mizutani T, Sekihara H. Expression of apoptosis on rat liver by hepatic vagus hyperactivity after ventromedial hypothalamic lesioning. Am J Physiol 280:G958–G967, 2001.
7. De Groot J. The rat hypothalamus in stereotaxic coordinates. J Comp Neurol 113:389–400, 1959.
8. Seliskar M, Rozman D. Mammalian cytochromes P450—importance of tissue specificity. Biochim Biophys Acta 1770:458–466, 2007.
9. Inui Y, Kawata S, Matsuzawa Y, Tokunaga K, Tamura S, Fukuda K, Maeda Y, Tarui S. Selective increase in cytochrome P450 content in hepatic microsomes from rats with ventromedial hypothalamic lesions. Int J Obes 15:221–225, 1991.
10. Turek FW, Belluardo N, Funakoshi H, Ibanez CF. Obesity and metabolic syndrome in circadian clock mutant mice. Science 308: 1043–1045, 2005.
11. http://genatlas.medecine.univ-paris5.fr/fiche.php?symbol=ELOVL6.
12. Wilson-Kubalek EM, Cheeseman IM, Yoshioka C, Desai A, Milligan RA. Orientation and structure of the Ndc80 complex on the microtubule lattice. J Cell Biol 182:1055–1061, 2008.
13. Romao M, Tanaka K, Sibarita JB, Ly-Hartig NT, Tanaka TU, Antony C. Three-dimensional electron microscopy analysis of ndc10–1 mutant reveals an aberrant organization of the mitotic spindle and spindle pole body defects in *Saccharomyces cerevisiae*. J Struct Biol 163:18–28, 2008.
14. Stout-Delgado HW, Getachew Y, Miller BC, Thiele DL. Intrahepatic lymphocyte expression of dipeptidyl peptidase I-processed granzyme B and perforin induces hepatocyte expression of serine proteinase inhibitor 6 (Serpinb9/SPI-6). J Immunol 179:6561–6567, 2007.
15. Vercammen D, Belenghi B, van de Cotte B, Beunens T, Gavigan JA, De Rycke R, Brackenier A, Inze D, Harris JL, Van Breusegem F. Serpin1 of Arabidopsis thaliana is a suicide inhibitor for metacaspase 9. J Mol Biol 364:625–636, 2006.